An investigation of the evolution of the beach zone of the St Georgios bay (Naxos island, Aegean Sea), in relation to its morphological and hydrodynamical characteristics

ELEFTHERIOU K.[1], EVELPIDOU N.[1], POULOS S.[1], ANDRIS P.[1], VASSILOPOULOS A.[1]

ABSTRACT

The shallow bay of St. Georgios is situated in the northwestern part of the Naxos Island and it is characterized by a 2.7 km long sandy coast consisting of fine-grained (sandy) material. Sand dunes are the landward limit of the beach zone, whilst at the southwestern part of the coast an extensive lagoon plain has been formed. A partially emerged reef and the morphologically associated Manto islet protect the middle and southwestern part of the beach zone from the most frequent (>40% annually) incoming N waves and the highest NW waves (>3 m).

The coastal zone is under erosion as shown by the reduction in size (>50%) of the Manto islet and the extensive erosion of the foredunes, despite the reduction of the incoming wave energy due to the reef presence. The continuous erosion (lowering) of the reef in connection with the expected eustatic sea level rise is anticipated to cause further retreat of the shoreline, demolishing the sand dune field and inundating the nearby low-lying hinterland area.

Keywords: coastal geomorphology, shoreline changes, coastal erosion, inundation, sand dunes, sea level change.

1. INTRODUCTION

The eustatic sea level changes have played a predominant role in the evolution of the coastal zone in the Cyclades Islands considering the relatively low tectonic activity of the Attiko-Cycladic massif (Bonneau et al., 1978; Keay et al., 2001; Pe-Piper & Piper, 2002) (Fig. 1) to which they belong. Hence, coastal morphology has been strongly associated with the upper Holocene slow rate (<1 mm/year) of sea level rise (Poulos et al., 2009) which has been recently enhanced, accounting for some 18 cm for the period 1890-1990 (Warrick et al., 1996).

It will be further affected by the future potential sea-level rise of approximately 38 cm (moderate scenario), according to the latest IPCC report (2007).

The scope of the present study is to examine the evolution of the coastline of St Georgios bay in relation to its geomorphological and hydrodynamic characteristics, whilst special emphasis is placed upon its morphological response to the predicted future sea level rise.

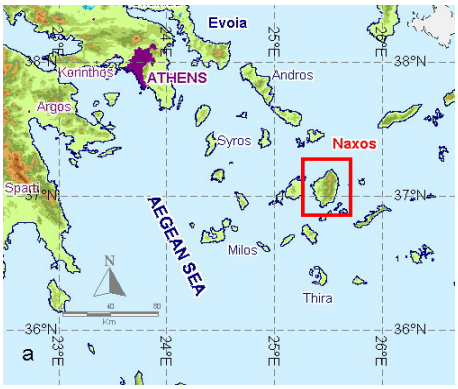

Figure 1: Geographical location of the Naxos Island

[1]*National & Kapodistrian University of Athens, Faculty of Geology & Geoenvironment, Department of Geography and Climatology Panepistimioupolis, Zografou, 15784, Athens*

Table 1: Offshore wave direction and height expressed in percentage of annual occurrence (after Athanasoulis & Skarsoulis, 1992).

Direction	N	NE	E	SE	S	SW	W	NW	Calm
(%)	21.8	8.2	5.7	4.7	3.3	7.6	24.7	20.0	4.0
Height (m)	0-0.5	0.5-1	1-1.5	1.5-2	2-2.5	2.5-3	3-4	4-5	>5
(%)	36.6	24.1	17.1	9.3	5.8	3.3	2.6	0.8	0.4

2. THE STUDY AREA

St Georgios coastal zone is located at the NW coast of Naxos Island, at a distance of few km from the homonymous city. It consists of three concave beach zones separated from a small headland and being sheltered by a small island, named Manto, and a partially emerged reef (Fig. 1). A small elongated drainage basin (trending E-W) supplies the coastal zone of St. Georgios with terrigenous sediments. The backshore area of the St.Georgios beach zone is dominated by alluvial (mostly sandy) and lagoon deposits, which are mainly located behind the middle SW sector of the beach zone (Fig. 3). In addition, a sand dune field forms the natural boundary between the beach zone and the landwards alluvial deposits.

Waves approach from W, NW and N directions, with heights <1.5 m at an annual percentage of occurrence >60%, while waves higher than 5 m are rare (<0.4%) (Table 1).

3. METHODOLOGY

Sedimentological characteristics have been studied along three sections (one for each of the three beach sectors; Fig. 3) after the sampling and granulometric (σ_I: sorting; Sk_I: skewness) analysis (according to Folk, 1974) of thirteen (13) surficial sediment samples. For the morphological characteristics of the sub-aerial and subaqeous part of the St. Georgios beach zone two (2) long sections (approximately 3.7 and 5 km long, respectively) were drawn on the basis of topographic diagrams (1:5,000). The calculations of wave characteristics were based on the wind data obtained from the National Meteorological Service. The determination of the wave parameters, such as offshore significant height (H_s), period (T), length (L_o), closure depth (maximum depth where the subaqueous profile changes) (h_c), breaking wave height (H_b), breaking wave depth (d_b), wave power (Po), energy loss (kt) and maximum wave run-up height (R) was accomplished with the use of the following equations (CERC, 1984; Komar, 1998):

$$H_s = 5.112 * 10^{-4} W * F^{0.5}$$

$$Hb = 0.565 * H_s / [(H_s / L_0)^{\wedge} 0.5]$$

$$Eo = \rho * g * H_s^2 / 8$$

$$R = 0.36 * g^{0.5} * S * H_s^{0.5} * T$$

$$T = 6.238 * 10^{-2} * (W * F)^{0.33}$$

$$d_b = H_s / 0.78$$

$$P_0 = E_0 * (C_0 / 2)$$

$$h_c = 2.28 \; H_s - \left(\frac{H_s^2}{g \, T^2} \right)$$

where W is the wind speed (m/s), F is the effective wave fetch (m), g= 9.81 m/s^2, ρ=1025 kg/m^3, S is the coastal slope (tan), Hs is the offshore significant maximum wave height, Eo is the offshore wave energy (Joule/m) and Po the incoming wave power (W/m).

In particular, the percentage of wave energy loss ($k_t = H_t / H_s$), due to the breaking over a reef is given as the ratio between the transmitted significant wave height (Ht) and the incoming wave height (H_s). In the case of a submerged reef the values of the ratio k_t are related to the parameter H_s/gT^2 through the ratio d_s/d (Rambadu & Mani, 2005), where d_s is the depth of reef surface and d is the water depth seawards to

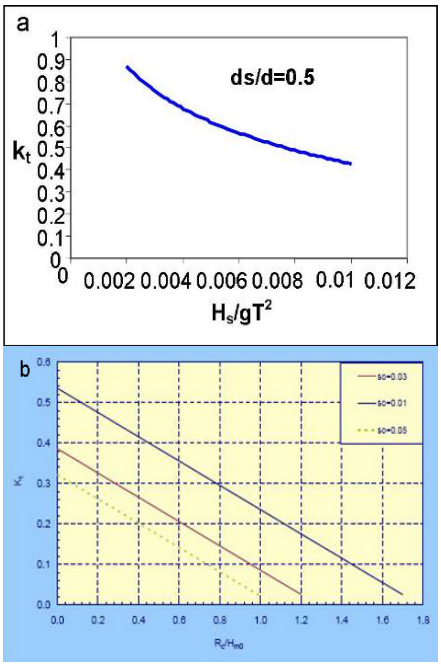

Figure 2: Diagram of energy loss over (a) a submerged reef and (b) an emerged reef

the reef while the incoming wave characteristics are presented by the ratio (Fig.2a).

In the case of an emerged reef, the k_t is derived from the diagram presented on Fig. 2b, which relates Kt with the ratio Rc/H_s (Pullen et al., 2007), where Rc is the reef height above mean sea level and H_s is the incoming wave height for waves of different steepness (so).

Finally, the overall morphology of the study coastal area has been investigated with the use and interpretation of aerial photographs, obtained from the Hellenic Army Geographical Service (HAGS). The aerial photographs of 1960 (1:30,000) and 1988 (1:33,000) were imported in a GIS following geo-referencing and compared in order to reveal coastline erosion, geographic extent of the various landforms (e.g. sand dunes) and future inundation of the backshore area due to future sea level rise.

4. RESULTS AND DISCUSSION

Morphological characteristics

The coastal zone of St Georgios has been developed within the homonymous bay having a shoreline of total length of 2.7 km. Further, it may be divided into three sub-regions (A, B and C). Besides, the southwestern sub-regions B and C are protected by an elongated reef (about 1.2 km in length) which extends almost parallel to the present day coastline. The largest part of the reef is raised above sea level a few tens of centimeters, with only its northeastern submerging up to 1 m below sea level. The material of the reef is sandy and probably constitutes a lithified pre-Holocene sand dune, denoting, therefore, the existence of an older (possibly Pleistocenic) coastline. The nearshore zone between the reef and the shoreline is particularly shallow, with depths not exceeding 2 m and being as much as 1.5 m for a distance of 100 m from the shoreline (Eleftheriou & Anagnostou, 2006). Nowadays, the Manto islet (Fig. 3) has been turned into a tombolo (Evelpidou, 2001) due to sediment accumulation at its lee (landward) side; the latter indicates that the longshore transport is from the north to south.

The northern and unprotected sector (sub-region A) of the coastal zone, whose shoreline length is 1 km (Fig. 3), presents a beach zone ranging between 14 and 36 m (Fig. 4; section 1). This sector is characterised by a total lack of dunes, most probably due to human interference, i.e. building activity. The middle sector (sub-region B) which incorporates a shoreline with length of 800 m (Fig. 3) presents a very narrow sub-aerial part of no more than 5 m width (as shown on Fig. 4; section 2).

The dunes (with sparse and low vegetation) in this sector reach elevations of 2-4.5 m, whilst they extend landward to more than 120 m. A main characteristic of the dune fields is the extensive and intensive erosion of the foredunes. Finally, the southwestern sector (sub-region C), having a shoreline length of 830 m (Fig. 3), is characterized by a wider subaerial part of its beach zone of approximately 140 m, while the dune field having average elevations up to 3.5 m extends landwards to a distance of 60 m (Fig. 4; section 3). Moreover, this part of the coastal zone is associated seawards with the Manto islet and landwards with a dune field that separates the beach zone from a rectangular low-lying alluvial plain, filled with lagoon deposits.

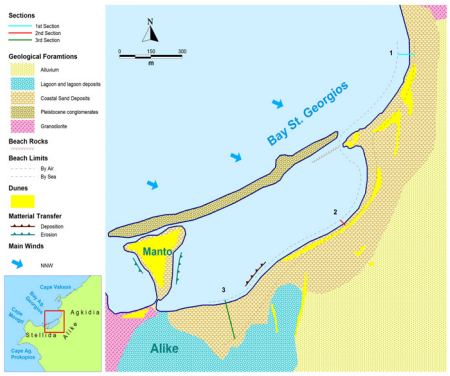

Figure 3: The geomorphology of the coastal zone of St. Georgios bay (1, 2, 3 : studied sections)

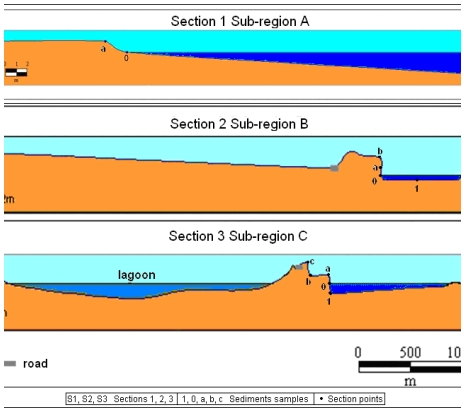

Figure 4: Schematic presentation of the topographical sections 1, 2 and 3 of the beach zone and the morphological characteristics of the coastal zone along the sections 2 (length ~4950 m) and 3 (length ~3752 m) in the sub-regions B and C, respectively.

5. GRANULOMETRY

The grain size analysis of the samples collected along the sections 1, 2 and 3 (Table 2), reveals the sandy character of the deposits, whose texture varies from sand (S: <1 φ) to slightly gravelly sand ((gS): 1-2.2 φ). Most of the samples are moderately shorted with variable skeweness, indicating hydrodynamic variability. For the same reasone, the shoreface samples present relatively coarser material. Furthermore, the sediments from sub – region A, generally present good sorting and more negative skewness in comparison to those of the sub-regions B and C (Table 2); this is attributed to the fact that these two sub-regions (B and C) receives reduced wave energy flux, as they are protected by the reef-Manto islet complex. Furthermore, the similarity in grain size distribution (either texture and/or Mz) between the subaqueous (i.e. From a water depth of -1 m) samples and those obtained from the fore-dunes, in all sub-regions (A, B and C) indicates that nearshore shallow area consists of sedimentary material, originating from the same source and that the dune material originates from the nearshore region, as it happens usually.

Wave regime

The offshore characteristics of the wind-induced waves approaching from the N, NW and W are listed in Table 3.

Although the most frequent incoming waves, on an annual basis, are generated by the north winds (f=43.2%), the highest waves (H_s>3 m) may approach only from the NW due to longer wave fetch (Table 3). Subsequently, the total annual amount of wave energy flux (Po) from the NW is about three times higher than that coming from the N and at least one order of magnitude higher than that coming from W. Moreover, the largest incoming waves can mobilise the seabed sediment (h_c) up to 7 m water depth, while they break at a depth of approximately 3 m. The run-up ability of the incoming waves (Table 4) on the unprotected sub-region A reaches an elevation of 3.2 m in the case of NW winds, while for the N and W winds the elevations are much smaller, i.e. 0.8 m and 0.3 m, respectively. In the case of the protected from the reef sub-regions B and C, where the incoming wave energy is reduced by 50-56%, the run–up ability is smaller, i.e. about 2 m for the NW, 0.65-0.80 m for the N and <0.3 m for the W incoming waves.

In autumn 2007, wave run-up height in sub-region B was measured at 0.6 m, which corresponds to a transmitant wave height (H_t) of approximately 0.73 m (reformed after its passage and break on the reef); the latter is related to an offshore incoming significant wave height of 1.3 m ($H_s = H_t/k_t$) that may have been induced by a

Table 2: Grain-size statistical analysis results according to Folk (1974) (for sample location see Figure 4).

	Mz (φ)	Texture	Sorting		Skewness	
Section 1						
S1-b	1.86	S	0.31	very well sorted	-0.11	coarse-skewed
S1-a	1.91	S	0.28	very well sorted	-0.12	coarse-skewed
S1-0	1.37	(g)S	0.94	moderately sorted	-0.61	strongly coarse-skewed
S1-1	1.89	S	0.31	very well sorted	-0.15	coarse-skewed
Section 2						
S2-b	1.02	S	0.94	moderately sorted	-0.47	strongly coarse-skewed
S2-a	1.59	(g)S	0.55	moderately well sorted	-0.13	coarse-skewed
S2-0	1.02	(g)S	0.85	moderately sorted	-0.32	strongly coarse-skewed
S2-1	2.23	(g)S	0.97	moderately sorted	+0.26	fine-skewed
Section 3						
S3-c	1.32	(g)S	0.97	moderately sorted	-0.47	strongly coarse-skewed
S3-b	1.38	(g)S	0.67	moderately well sorted	-0.34	strongly coarse-skewed
S3-a	1.69	S	0.31	very well sorted	+0.36	strongly fine-skewed
S3-0	0.40	S	0.61	moderately well sorted	+0.40	strongly fine-skewed
S3-1	1.58	(g)S	0.60	moderately well sorted	-0.26	coarse-skewed

Table 3: The calculated wave characteristics (U: wind speed; f: wind frequency; T: wave period; H_s: significant wave height; h_c: closure depth; H_b: breaking wave height; d_b: breaking depth; C_o: offshore wave speed; E_o: offshore wave energy; P_o: offshore wave power).

U	*f*	*T*	H_s	h_c	H_b	d_b	C_o	E_o	P_o
(m/s)	*(%)*	*(sec)*	*(m)*	*(m)*	*(m)*	*(m)*	*(m/sec)*	*(Joule/m²)*	*(Watt/m)*
N (F=40.5 km)									
2.0	1.70	0.80	0.02	0.05	0.48	2.18	1.25	0.66	0.07
5.0	4.57	2.50	0.22	0.50	1.66	5.86	3.90	60.83	380.83
8.5	6.16	3.67	0.59	1.34	2.56	7.89	5.73	437.53	21220.24
13.5	8.82	4.43	1.04	2.37	3.83	11.30	6.91	1359.47	293052.27
19.0	6.79	5.09	1.58	3.59	3.38	8.71	7.94	3137.74	2034700.28
24.5	15.13	5.65	2.16	4.91	6.83	19.40	8.81	5864.22	8641424.57
Sum	43.16								10990778.27
W (F=9 km)									
2.0	0.16	0.80	0.02	0.05	0.07	0.21	1.25	0.50	0.05
5.0	0.31	1.80	0.14	0.32	0.17	0.39	2.81	24.64	98.11
8.5	0.306	2.24	0.28	0.64	0.19	0.38	3.49	98.54	2266.91
13.5	0.26	2.70	0.49	1.11	0.20	0.34	4.21	301.78	30630.67

19.0	0.10	3.10	0.74	1.68	0.10	0.13	4.84	688.28	208887.45
24.5	0.11	3.40	1.02	2.32	0.11	0.14	5.30	1307.69	909125.36
Sum	1.24								1151008.55
NW (F=88 km)									
2.0	0.44	0.80	0.02	0.05	0.16	0.56	1.25	0.50	0.05
5.0	0.93	2.47	0.22	0.50	0.46	1.19	3.85	60.83	380.82
8.5	1.03	4.75	0.86	1.96	0.66	1.32	7.41	929.61	65735.54
13.5	0.97	5.73	1.53	3.48	0.71	1.25	8.94	2.942.29	933348.43
19.0	0.94	6.58	2.33	5.30	0.75	1.21	10.26	6.823.62	6527344.27
24.5	2.53	7.29	3.18	7.23	1.76	3.24	11.37	12.710.34	27584038.63
Sum	6.84								35110847.73

Table 4: Estimation of wave run-up (R) in the case of no-reef presence, a submerged (-1m) and an emerged (+0.2m) reef.

Wind	*N*			*NW*			*W*		
U(m/s)	*Et(m)*	*Ht(m)*	*Rt(m)*	*Et(m)*	*Ht(m)*	*Rt(m)*	*Et(m)*	*Ht(m)*	*Rt(m)*
Case 1: Without the reef (k_t=1)									
2.0	0.66	0.02	0.01	0.50	0.02	0.01	0.50	0.02	0.01
5.0	60.83	0.22	0.11	60.83	0.22	0.11	24.64	0.14	0.07
8.5	437.53	0.59	0.27	929.61	0.86	0.43	98.54	0.28	0.11
13.5	1359.47	1.04	0.44	2942.29	1.53	0.68	301.78	0.49	0.18
19.0	3137.74	1.58	0.62	6823.62	2.33	0.97	688.28	0.74	0.26
24.5	5864.22	2.16	0.80	12710.34	3.18	1.26	1307.69	1.02	0.33
Case 2: Submerged reef (-1 m) for ratio ds/d=0.5 and H_s/gTp^2=0.0065 then K_t= 0.56									
2.0	0.29	0.02	0.01	0.22	0.01	0.01	0.22	0.01	0.01
5.0	26.77	0.15	0.09	26.77	0.15	0.09	10.84	0.09	0.05
8.5	192.51	0.39	0.22	409.03	0.57	0.35	43.36	0.19	0.09
13.5	598.17	0.69	0.36	1294.61	1.01	0.56	132.78	0.33	0.15
19.0	1380.61	1.05	0.50	3002.39	1.55	0.79	302.84	0.49	0.21
24.5	2580.26	1.43	0.65	5592.55	2.11	1.02	575.38	0.68	0.27
Case 3: Emerged reef (+0.2 m) for ratio Rc/H_{m0}=0.1 then K_t= 0.50									
2.0	0.33	0.02	0.01	0.25	0.01	0.01	0.25	0.01	0.01
5.0	30.42	0.16	0.10	30.42	0.16	0.09	12.32	0.10	0.05
8.5	218.76	0.42	0.23	464.80	0.61	0.36	49.27	0.20	0.10

13.5	679.73	0.74	0.37	1471.15	1.08	0.58	150.89	0.35	0.15
19.0	1568.87	1.12	0.52	3411.81	1.65	0.82	344.14	0.52	0.22
24.5	2932.11	1.53	0.67	6355.17	2.25	1.06	653.84	0.72	0.28

N and/or NW wind with speed >10 m/sec (Table 3). Therefore, during storms the beach zone experiences more intensive (erosive) wave conditions as indicated by the maximum predicted run-up heights (>1 m).

Recent and future coastal zone evolution

A series of aerial photos, from 1945 to 1997, and extensive field work from 1999 to 2007, reveal remarkable morphological changes in the coastal zone of St Georgios bay, which are particularly profound in the area around the ex-Manto islet. The later island and its neighbouring reef due to their sedimentary character have severely eroded as shown by the aerial photographs of 1960 and 1988 (Fig. 5 a, b). The surface area of the island has been substantially decreased by ~53% (Evelpidou, 2001) during the aforementioned time period. Also, coastline retreat is observed in the small headland which separates sub-region B from C, as well as in the beach zone and associated dunes lying along the coastline of these two sub–regions. In fig. 6, the consequences from the erosion appear in an emphatic way, with the with the foredune field displaying serious losses. Such extensive erosion phenomena do not occur frequently at the moment but only under storm events, like the one took place on january 2004, associated with wind speeds >110 km/h (Nastos et al., 2006). Furthermore, the 'lost' material from the beach zone seems to have been contributed to the transformation of the manto islet into a tombolo (Fig. 5d); the latter assumption is supported by the similarity in grain-size distributions between the sediment samples collected from the area between the reef and the shoreline and those taken from the near by foredunes (as discussed earlier).

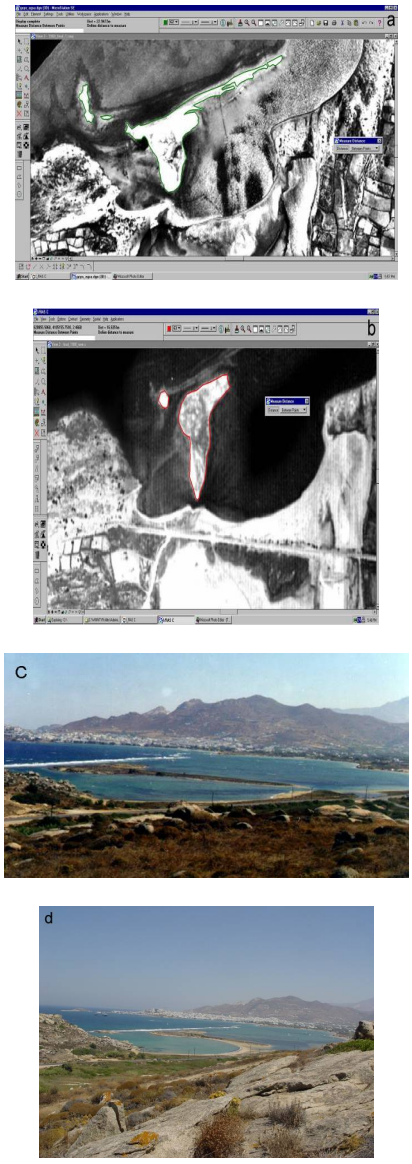

Figure 5: Aerial photographs of (a) 1960 and (b) 1988 and photographs taken in (c) 2000 and (d) 2007

Figure 6: The fore-dune area in sub-region B in (a) summer 2003 and (b) in late autumn 2007

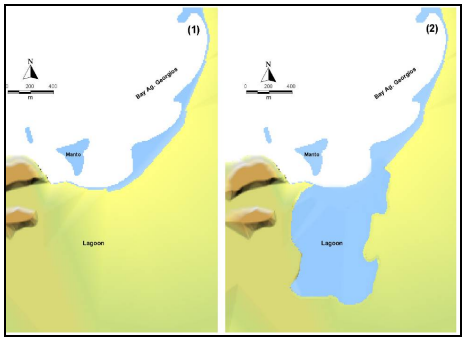

Figure 7: Schematic presentation of the expected evolution of St Georgios coastal zone before and after the dunes erosion.

The assessment for the future evolution of St Georgios coastal zone is rather pessimistic due to the observed eustatic rise of sea level during 1989-1990 (18 cm) and the estimate for a further rise 38 cm until 2100 according to the latest IPCC report (2007) on global climatic change. Moreover, this report is also referred to an increased frequency of extreme weather events, like the one mentioned earlier (in January 2004). Thus, the expected rise of sea-level rise together with the increased occurrence of storms may be catastrophic for the study coastal area, as these phenomena will intensify the erosive capacity of the incoming waves due to larger nearshore water depths and the further erosion of the existing reef. This will lead to higher wave run-up heights in sub-regions B and C, analogue to those occurring in the unprotected sub-region a, hence being capable to erode (remove) the total volume of the foredunes. According to this scenario, the shoreline will retreat tens of meters landwards, while the low-lying areas, (e.g. the occurring lagoon) will be inundated (this is shown schematically in Fig. 7). Overall, the coastal zone is under an erosional status, as shown by the reduction in size (>50%) of the ex-Manto islet and the severe erosion of the foredunes, despite the reduction of the incoming wave energy due to the presence of the reef.

The wave-induced erosion phenomena will be enhanced by the unceasing erosion of the reef, the overcoming sea-level rise, and the rather frequent future occurrence of storms; this will bring about an overall retreat of the shoreline, causing the destruction of the sand dune field and inundation of the low-lying hinterland area (e.g. lagoon).

Acknowledgements

Mrs A. Eleftheriou thanks Dr Ch. Anagnostou (HCMR) for his initial involvement in the survey of this coastal area. The authors are grateful to Mr G. Alexandrakis for his assistance in the study of the wave climate, while part of the expenses regarding Ass. Prof. S. Poulos covered by the Kapodistrias project (NKUA No. 70/4/7618).

REFERENCES

Athanasoulis, G. and Skarsoulis, E., 1992. *Wind and Wave Atlas of north-east Mediterranean Sea*, Laboratory of Nautical and Marine Hydrodynamics, NTUA, Athens

Bonneau, M., Geyssant, J. and Lepvrier, C., 1978. *Tectonique Alpine dans le Massif d' Attique-Cyclades (Gréce): Plis Couchés ki-*

lométriques dans l' île de Naxos, Revue de Géographie et de Géologie Dynamique, Masson Éditeur, Deuxiéme série, Vol. XX, pp. 109, 114.

CERC (1984) *Shore protection Manual*, U.S. Army Corps of Engineers Coastal Engineering Research Center, Washington.

Eleftheriou, K. and Anagnostou, Ch., 2006. *Morphological condition and drift of the Saint George sandy coast in Naxos island (poster*), 8th Hellenic Symposium of Oceanography and Fishery, Abstracts, pp.175.

Evelpidou, N., 2001. *Geomorphologic and environmental observations in Naxos island, with utilization of tele-tracing and GIS methods,* PhD Thesis, Department of Geography and Climatology Faculty of Geology, University of Athens, pp. 118-120.

Folk R.L., 1974. *Petrology of Sedimentary Rocks*, Hemphill Publishing Company, Texas, pp. 183.

IPCC (Intergovernmental Panel on Climate Change), 2007. *Climate Change 2007: The physical science basis*, Contribution of Working Group I to the fourth assessment report of the Intergovernmental Panel on Climate Change, Cambridge University Press, Cambridge.

Keay, S., Gordon, L. and Buick, I., 2001. *The timing of partial melting, Barrovian metamorphism and Granite intrusion in the Naxos metamorphic core complex*, Cyclades, Aegean Sea, Greece, Tectonophysics, 342, pp. 276-278, 280, 287, 293-294.

Komar, P.D., 1998. *Beach processes and Sedimentation* (2nd edition), Prentice Hall, New Jersey, pp. 544.

Nastos, P.T., Drakopoulos, P. and Poulos, S., 2006. *The meteorological bomb on 22 January 2004 at Aegean Sea, Greece and its impact on sea level*, 6th Annual Meeting of the European Meteorological Society / 6th European Conference on Applied Climatology, Slovenia.

Pe-Piper, G. and Piper, J.W., 2002. *The igneous rocks of Greece: The anatomy of an Oregon*, Gebrüder Borntraeger-Berlin-Stuttgart, pp. 79, 310, 313-316.

Poulos, S.E., Ghionis, G. & Maroukian H., 2009. *Sea-level rise trends in the Attico-Cycladic region (Aegean Sea) during the last 5000 years*, Journal of Geomorphology, 107(1-2), pp. 3-9.

Pullen, T., Allsop, N.W.H., Bruce, T., Kortenhaus, A., Schuttrumpf, H. and Van der Meer, J.W., 2007. *Wave overtopping of sea defenses and related structures*: Assessment Manual, Environmental Agency, UK, pp.185 (www.overtopping-manual.com).

Rambadu, A.C. and Mani, J.S., 2005. *Numerical prediction of performance of submerged breakwaters*, Ocean Engineering, 32, pp. 1235-1246.

Warrick, R.A., Le Provost, C., Meier, M.F., Oerlemans, J. and Woodworth, P.L., 1996. *"Changes in sea level"*, In: J.T. Houghton, L.G. Meira Fihlo, B.A. Callander, N. Harris, A. Kattenberg and K. Maskell (eds) "Climate Change 1995: The Science of climate Change", Contribution of WGI to the Second Assessment report of the Intergovernmental panel on Climate Change. Cambridge University Press, Cambridge, pp. 359-405.